LOW TEMPERATURE PROPERTIES OF GLASSES

by

Eric Ralph Grannan

LOW TEMPERATURE PROPERTIES OF GLASSES

A Dissertation

Presented to the Faculty of the Graduate School

of Cornell University

in Partial Fulfillment of the Requirements for the Degree of

Doctor of Philosophy

by

Eric Ralph Grannan

January 1989

© Eric Ralph Grannan 1989

ALL RIGHTS RESERVED

BIOGRAPHICAL SKETCH

Eric Grannan graduated from Caltech in 1984.

To my parents

ACKNOWLEDGMENTS

I have never really understood acknowledgments until now. I had always thought that they were either an obligation, in which case they didn't really mean anything, or they were just showing off — look how magnanimous I am! As I look back on my years in graduate school, however, I realize how indebted I am to so many people, and it is honestly a pleasure to be able to thank them.

First of all I would like to thank my advisor, Jim Sethna. I do not think that anyone could have asked for a better teacher and helper. He has great physical and mathematical insight and many times has helped me to see to the heart of a matter. I have learned that even when he says something that sounds foolish, it is best to think about it very hard, because it almost always turns out that he was right all along. His kindness and enthusiasm have made Cornell a much more pleasant place to be.

I would like to thank Mohit Randeria, who as well as being a good friend, has worked with me on this project for almost two years now. It has been a pleasure working with him, and I promise to return *Phonon Scattering in Condensed Matter V* very soon now.

I would also like to thank the rest of the Sethna group. Dan Rokhsar, with whom I spent some marvelous months in Santa Barbara. Steve Langer who has always enlivened the computer room, as well as being not too begrudging about modifying his INTER program (and now axis!) for me. Jean Carlson, volleyball player and procurer of books. Ming (it is not that we don't like...) Huang, sharer of the fridge. Chris Dogbread Myers – Hahn! Banach! Get your lazy butts in here and do some work! And of course, I can't neglect our two younger members,

Shelly Shumway and Joel Shore.

Arthur Smith, the most powerful integrating machine known to man, has been extremely kind and helpful, what with bergamot, integrating, and spending a whole night getting psfig working.

Finally, I want to thank my fellow members of Fleming East: Mignon Belongie, Steve Jones, John Sahr, and Ned Wingreen,for helping to make Ithaca an almost bearable place. May your tendrils always wave.

TABLE OF CONTENTS

		Page
Chapter 1	Introduction	1
Chapter 2	Motivating the Model	4
Chapter 3	Elasticity	7
3.1	Introduction	7
3.2	Review of Elasticity and Notation	9
3.3	Traditional Elasticity	10
3.3.1	Point Defects in Elastic Media	11
3.3.2	Real Space, Isotropic Medium	12
3.4	Fourier Space Green's Function by Minimization	14
3.4.1	Periodic Strain Fields	16
3.4.2	Full Hamiltonian	19
3.4.3	The Elastic Fields of Point Forces and Dipoles	21
3.4.4	Isotropic Elastic Constants	24
3.4.5	Cubic Elastic Constants	25
3.4.6	Interaction Energy	27
3.4.7	External Stresses	29
3.5	Cutoffs	31
Chapter 4	Numerical Stuff	41
4.1	Introduction	41
4.2	The Simulation	42
4.3	Ground State Structure	45
4.3.1	Non-Diluted Systems	47
4.3.2	Diluted Systems	48
4.4	Barrier Heights	51
4.4.1	Bare Barrier Heights	54
4.4.2	Relaxed Barrier Heights	63
4.5	Simulation with Cubic Elastic Constants	68
Chapter 5	Harmonic Stuff	69
5.1	Introduction	69
5.2	Normal Modes	70
5.3	Response to Static Fields	72

5.4 Finite Frequency Response 81
5.4.1 Phonon–Libration Coupling 81
5.4.2 Frequency Dependent Elastic Constants 84
5.4.3 Phonon Scattering 86
5.5 Universality of Softening and Plateau 88

Chapter 6 Comparison to Experiment 91
6.1 Introduction 91
6.2.1 Numbers 91
6.2.2 Specific Heat – Total Density of Harmonic Excitations . . 92
6.2.3 Thermal Conductivity 93
6.3 KBr:KCN 95
6.3.1 Low Temperature Thermal Properties – KBr:KCN 96
6.3.2 Dielectric Loss 99
6.4 Real Glasses, Vitreous Silica 110

Chapter 7 Other Theories, and Conclusions 114
7.1 Relation to Other Theories 114
7.2 Conclusions 118

Chapter 8 Entropy 121
8.1 Introduction 121
8.2 Entropy Determination 121
8.2.1 High Temperature 123
8.2.2 Low Temperature 124
8.2.3 Entropy of the Simulation 124

Appendix A Heat Bath 129
Appendix B Real Numbers 132
Appendix C Isotropic Minimum Energy Configuration 135
Appendix D Susceptibility 138

References 143

LIST OF TABLES

		Page
Table 1	Polynomial Cutoff Functions	37
Table 2	Ratio of Width to Peak Position for . . . . . Experimental and Simulation Barriers	62
Table 3	Coefficients of Linear Fits to Barriers	65
Table 4	Bulk Modulus of $KBr_{(1-x)}KCN_x$ as a function of concentration	80
Table 5	Parameters used in calculations . . . . . of thermal conductivity and specific heat	96

LIST OF FIGURES

		Page
3.1	Polynomial Cutoff	39
3.2	Exponential Integral Cutoff	40
4.1	Tee's Are Frustrated	46
4.2	Ground State Orientations	49
4.3	Orientational Correlations, $x = 0.25$	50
4.4	Orientational Correlations, $x = 0.5$	51
4.5	Orientational Correlations, $x = 0.7$	52
4.6	Barrier Height Distribution for Uncorrelated Dipoles	56
4.7	Barrier Height Distribution, $x = 0.1$	57
4.8	Barrier Height Distribution, $x = 0.25$	58
4.9	Barrier Height Distribution, $x = 0.5$	59
4.10	Barrier Height Distribution, $x = 0.7$	60
4.11	Barrier Height as a Function of Number of Near Neighbors	63
4.12	Mean of Barrier Height as Function of Near Neighbors	64
5.1	Density of Libration States	71
5.2	Participation Ratios, Various System Sizes	73
5.3	$\overline{A^2}(\Omega)$ Coupling to Long Wavelength Phonons	78
6.1	Density of libration mode states, phonon states	100
6.2	Scattering rate	101
6.3	Frequency Dependent Speed of Sound	102
6.4	Thermal Conductivity for $x = 0.25$	103
6.5	Thermal Conductivity for $x = 0.5$	104
6.6	Thermal Conductivity for $x = 0.7$	105
6.7	Specific Heat for $x = 0.25$	106
6.8	Specific Heat for $x = 0.5$	107
6.9	Specific Heat for $x = 0.7$	108
6.10	Barrier Heights from Dielectric Loss and Simulation	109
6.11	Low Frequency Modes, Vitreous Silica and Simulation	111
6.12	Thermal Conductivity of SiO_2 and the model	112
6.13	Specific Heat of SiO_2 and the model	113
8.1	Energy as a function of temperature on cooling, heating	125
8.2	Thermodynamic bounds on the entropy and statistical entropy	126
8.3	Number of local energy minima for small system	127

CHAPTER I — INTRODUCTION

Until about 1971, most physicists would have probably thought that glasses at low temperatures would behave much like crystals. Phonons of long enough wavelength would simply average over the disorder. Ziman stated in 1960[1] that "the waves ride over the irregularities, whose scale is only of the order of the correlation length L. The longer the wavelength, the less the wave sees of the irregularity, and the less it is scattered." He predicts that the mean free path would scale as $1/k^2$, and assuming, I think, (although he doesn't explicitly say so) a Debye specific heat proportional to T^3, predicts a thermal conductivity that is linear in temperature.

These peaceful days came to an end in 1971, when Zeller and Pohl[2] showed conclusively that glasses at low temperatures behave very differently from crystals. They reviewed available data, as well as their own work, and demonstrated that many quite different glasses behaved remarkably similarly at low temperatures.

At very low temperatures, below about 1 K, the thermal conductivity (Λ) of glasses is proportional to T^n, where n is approximately 1.8. The magnitude of the thermal conductivity is much smaller than in crystalline solids. At these same temperatures the specific heat C varies approximately linearly with temperature (actually with an exponent somewhat greater than one), in sharp contrast to the Debye prediction. Not only is there a linear contribution, but the specific heat can be parametrized by $AT + BT^3$, and when this is done, the value of B is generally (although not always) significantly larger than the Debye contribution predicted by the elastic constants. This is known as the "excess" specific heat.

Above these temperatures A levels off and enters a temperature independent regime called the "plateau", at around 10 K, before increasing again above this temperature. This plateau has been seen in many types of glasses and disordered materials, including structural glasses such as vitreous silica (window glass), glassy crystals (KBr:KCN), polymer glasses, and neutron irradiated quartz. A striking feature is that besides having a similar functional form, the magnitude of the thermal conductivity of a wide variety of glasses only varies by a factor of three or so in the low temperature regime; this is much smaller than the comparable variation in crystalline materials.

If one plots C/T^3, the curve actually does not fit $AT + BT^3$ very well, but exhibits a "bump", generally at about the same temperature as that of the plateau.

One can, as we have done above, distinguish two regimes in the behavior of glasses at low temperatures. There may, of course, be no fundamental justification for this distinction, but for the purposes of this paper we will take this perspective. The "low" temperature regime (below about 1 K) is characterized by the T^2 thermal conductivity, and the linear specific heat. The "intermediate" temperature regime (from about 1 to 20 K) is characterized by the plateau in the thermal conductivity and the bump in C/T^3. To avoid confusion, we should mention that there is a third, high temperature regime in glasses involving the glass transition about which we will say nothing.

Much theoretical work has been devoted to trying to explain the universal properties of glasses. The low temperature properties can be explained, at least at a phenomenological level, by the tunneling system model proposed by Anderson, Halperin, and Varma; and independently by Phillips[3,4].

This model postulates that since glasses are disordered, there will be atoms or groups of atoms that can exist in more than one stable configuration. This is modeled as a particle living in a double well potential. Assuming that the distribution of asymmetries is constant at zero asymmetry, this model leads to a linear specific heat, and a T^2 thermal conductivity. For a review of the tunneling system model, see the article by Phillips[5].

The higher, intermediate temperature properties, between about 1 and 20 K, have so far resisted a satisfactory theoretical explanation. These are the properties which I will address in this thesis. We will discuss other theories for these properties, and compare them to this model in chapter 7.

CHAPTER II — MOTIVATING THE MODEL

In very general terms, our model pictures glasses as consisting of defects of some sort, which interact with each other. We will assume that their strongest interaction is through their strain fields. In the absence of a symmetry that forbids it, the strain field that dies away most slowly with distance is that due to the elastic dipole moment. Therefore, a simple model for a defect in a medium is an elastic dipole.

The source for displacements in an elastic medium is a force concentrated at a point. In analogy with an electric dipole, an elastic dipole is given by two opposing forces whose strength goes to infinity as their separation goes to zero.

An elastic dipole is characterized by a symmetric tensor of rank two. We make three simplifying assumptions from a general model involving elastic dipoles, two of which are probably harmless, and one of which may have some substance. These assumptions are good for $KBr_{(1-x)}KCN_x$, the material that was the inspiration for the model.

First, we will consider traceless defects, which means that there is no volume change due to the dipole. This is a very good approximation in KBr:KCN, where the lattice constant is essentially constant as x is varied (for $x \lesssim 0.6$; above this concentration the material has a ferroelastic phase transition at low temperatures). Second, we restrict ourselves to the case where two of the axes are equal. Given these assumptions, only one number, Q_0, the elastic dipole moment, is needed to characterize the defect. The elastic dipole is then given by $Q_{ij} = Q_0(\hat{n}_i\hat{n}_j - \frac{1}{3}\delta_{ij})$, where $\hat{n}$ is a unit vector. This gives a dipole which can be pictured as looking something like an American football placed in a hole in

a block of rubber. It pushes out in one direction, and pulls in in the other two directions. As we define it, the elastic dipole has units of energy and couples to the strain field in the host medium.

Our third, more serious assumption, is that we neglect any interaction of the dipole with the crystal field. An isolated dipole in our model behaves like a free symmetric rotor. In KBr:KCN, the crystal field is small compared to the elastic interactions at the concentrations we are studying, but in general this is not the case. In general, a defect in an amorphous material will have preferred orientations.

At low temperatures the dipoles in our model freeze into a frozen configuration. We think that the small angular oscillations about this configuration are important for the low temperature properties. In this practically frozen state, it may not matter qualitatively whether or not the local orienting potential comes solely from interactions with other dipoles, or whether there is a sizable contribution from the local field.

We will compare our results with experimental data both on the glassy crystal KBr:KCN and on vitreous silica. In KBr:KCN, which was the original motivation for the model, we make the obvious association between elastic dipoles and cyanide ions, and we can get the microscopic parameters from experiment. These parameters are the elastic dipole moment, the moment of inertia, the density of defect modes, and the elastic constants, from experiment. In vitreous silica, we can still get the parameters from experiment, although at a phenomenological level, by adjusting them so that we can fit a measured density of harmonic states[6], as described below. At this point we do not have a microscopic justification for treating the material as interacting dipoles, although there may be some specific

degree of freedom which acts as a dipole defect[7].

We should emphasize that in this paper we assume the existence of tunneling systems when making fits to experimental data. Since experimentally only about 1 in 100,000 atoms is in a tunneling center, we do not expect to see too many in our simulation. We discuss this briefly in chapter 7.

CHAPTER III — ELASTICITY

3.1 Introduction

Ultimately, we want to simulate a disordered system of elastic dipoles. In general, second rank tensors will interact through a Hamiltonian of the form

$$\sum_{\mathbf{x}\neq\mathbf{x}'} A_{ijkl}(\mathbf{x},\mathbf{x}')Q_{ij}(\mathbf{x})Q_{kl}(\mathbf{x}'), \tag{1}$$

and in specific, for elastic dipoles, A will be the strain field at $\mathbf{x}$ caused by a dipole at $\mathbf{x}'$. The main question for this chapter is to determine A.

In the first few sections of the chapter, we will consider the problem of a single force or dipole in an infinite continuum. We will use the equation of elastic equilibrium to obtain the strain field of a dipole, first in Fourier space, which can be done for arbitrary anisotropy, and then in real space, for an isotropic medium. This is not the whole story, however, since we do not want to simulate a few dipoles in an infinite medium, but rather an infinite medium containing a finite density of dipoles.

A natural way to take the thermodynamic limit of a moderately sized system is to use periodic boundary conditions, in which a computationally manageable system is considered to be a unit cell of an infinite periodic array. To consider the effects of a periodic system in a systematic way, we will reformulate the problem in sections 3.4, and write down a "full Hamiltonian" which includes the energy in the phonon modes. This is different from the standard method of elasticity, in which the phonons are always considered to be fully relaxed. We will rederive in this way the Fourier space equations for the strain field of a dipole. We will

see that besides the $1/r^3$ strain field around each dipole, minimizing the energy in the $\mathbf{k} = 0$ mode leads to a uniform strain field. This strain field vanishes for a single dipole in an infinite medium, but in a system with a finite density of dipoles it only costs a finite amount of energy per dipole. The uniform strain field is important since it can cause a ferroelastic transition to a state where there is a long wavelength deformation, and the dipoles all line up. It also must be treated correctly, even in the absence of a long wavelength deformation, if you want to look at the response of the system to external applied stresses.

The phonons then mediate an interaction between dipoles. We will recover an effective Hamiltonian between dipoles of form (1) by minimizing the energy in the phonon modes, and we will discuss the interaction between dipoles mediated by the phonons.

Finally, we will consider the convergence of the sums involved in calculating the strain fields. We don't know how to sum analytically the contributions to the strain field from all the images of a dipole, so we must cut off the interaction in some fashion. The sum can either be cut off in real space, where we are summing over the sites of the dipoles, or in Fourier space, where we are summing over $\mathbf{k}$ values. Both in real space or in Fourier space this must be done carefully. In real space the strain field of a dipole dies away as $1/r^3$ and we will find that using an abrupt cutoff can cause this to converge to an incorrect value. In Fourier space the Fourier transform of the strain field does not die away at large k values, so unless the sum is done carefully, it will not converge at all.

3.2 Review of Elasticity and Notation

Go home, get any book on elasticity,[8,9,10] and read it until they start talking about thin plates. Then come back.

I will follow the notation in Hirth and Lothe[10], denoting displacement by $\mathbf{u}$, strain by ϵ, and stress by σ. The elastic constant tensor is given by c_{ijkl}. In general, c_{ijkl} is symmetric under interchange of $i \leftrightarrow j$, $k \leftrightarrow l$, and $ij \leftrightarrow kl$ so that there are 21 independent elastic constants. An *isotropic* medium has only two independent elastic constants, and c_{ijkl} can be written as

$$c^{\text{iso}}_{ijkl} = \lambda \delta_{ij}\delta_{kl} + \mu \left(\delta_{ik}\delta_{jl} + \delta_{il}\delta_{jk} \right), \tag{2}$$

where λ and μ are the Lamé coefficients. Cubic crystals have three independent elastic constants, c_{1111}, c_{1122}, and c_{1212}. These are usually written as c_{11}, c_{12}, and c_{44}, respectively, so that

$$c^{\text{cub}}_{ijkl} = c_{12}\delta_{ij}\delta_{kl} + c_{44}\left(\delta_{ik}\delta_{jl} + \delta_{il}\delta_{jk} \right) + \left(c_{11} - c_{12} - 2c_{44} \right) \delta_{ijkl}, \tag{3}$$

where δ_{ijkl} is zero unless all of $\{ijkl\}$ are equal.

Thermodynamic stability gives constraints on the values of the elastic constants, since the energy of an unstrained medium should be a minimum. In particular, both the bulk modulus and the shear modulus must be positive. For an isotropic medium, this means that $\mu > 0$, and $\lambda + \frac{2}{3}\mu > 0$. For a cubic medium, $c_{11} > 0$, $c_{44} > 0$, and $\frac{1}{2}c_{11} + c_{12} > 0$.

I will denote partial derivatives with respect to x_i by ∂_i, so that

$$\frac{\partial^2 u}{\partial x_i \partial x_j} \equiv \partial_{ij} u, \tag{4}$$

for example. Summation over repeated tensor indices is implied in all equations. Arbitrary positions in the elastic continuum will be written as $\mathbf{r}$, locations of defects will given as $\mathbf{x}$. Vectors with hats, $\hat{\mathbf{k}} \equiv \mathbf{k}/k$, are unit vectors.

In this chapter we will be deriving Green's functions for the response of elastic media to point forces and dipoles. The notation is illustrated by the Green's function for the displacement field of a dipole, written as $u_{ijk}(\mathbf{r})$. The first index of u_{ijk} is the index of the displacement field, and the last two are contracted with the dipole Q_{jk}, giving a displacement field at $\mathbf{r}$ of

$$u_i(\mathbf{r}) = u_{ijk}(\mathbf{r} - \mathbf{x})Q_{jk}(\mathbf{x}). \tag{5}$$

In general, the first indices of a Green's function are the indices of the field to be calculated, and any remaining indices are to be summed over. For example, u_{ij} is the Green's function for the displacement field due to a force, and ϵ_{ijkl} is that of the strain field due to a dipole. Since the number of indices of the field is known, this cannot cause confusion. We shall sometimes write the real space Green's function for the strain due to a dipole, ϵ_{ijkl}, as J_{ijkl}. This is by analogy with spin systems, since it will turn out that the interaction energy between two dipoles is $-J_{ijkl}Q_{ij}Q_{kl}$. Note that the units of the Green's function are not the units of the field, since the Green's function still has to be multiplied by a source.

3.3 Traditional Elasticity

In this section we calculate the elastic fields by solving the equation of elastic equilibrium.

3.3.1 Point Defects in Elastic Media

A general way of determining the displacement field due to a distribution of forces in an elastic medium is to first calculate the response of the medium to a point force. This is analogous to calculating the electrostatic potential $V(\mathbf{r})$ of a given charge distribution by using the Green's function which solves Poisson's equation for a point charge,

$$\nabla^2 G(\mathbf{r}) = -4\pi\delta(\mathbf{r}) \qquad \Longrightarrow \qquad G(\mathbf{r}) = \frac{1}{r}. \tag{6}$$

For an elastic medium, the corresponding equation which we want to solve is

$$\partial_j \sigma_{ij} + F_i \delta(\mathbf{r}) = 0, \tag{7}$$

or

$$c_{ijkl}\partial_{jl} u_k + F_i \delta(\mathbf{r}) = 0, \tag{8}$$

writing out the σ_{ij}. The solution to this equation apparently can only be expressed analytically in real space for isotropic (Lord Kelvin) or hexagonal[11] (Lifshitz and Rozenzweig) media. The fact that it can be expressed analytically for a hexagonal medium maybe isn't terribly surprising since a hexagonal material is isotropic within a plane.

We can solve (8) in Fourier space by writing

$$\delta(\mathbf{r}) = \frac{1}{8\pi^3} \int e^{i\mathbf{k}\cdot\mathbf{r}}\, d\mathbf{k} \tag{9}$$

Then the response to a point force is:

$$\tilde{u}_{11} = \frac{1}{D}\frac{1}{Vk^2}\left[{c_{44}}^2\hat{k}_1^2 + c_{11}c_{44}\left(\hat{k}_2^2 + \hat{k}_3^2 - 2\hat{k}_2^2\hat{k}_3^2\right) + \left({c_{11}}^2 - {c_{12}}^2 - 2c_{12}c_{44}\right)\hat{k}_2^2\hat{k}_3^2\right] \tag{68}$$

$$\tilde{u}_{12} = \frac{1}{D}\frac{\hat{k}_1\hat{k}_2}{Vk^2}\left[(c_{12}+c_{44})\left(\hat{k}_3^2(2c_{44}+c_{12}-c_{11}) - c_{44}\right)\right]$$

The response to a dipole is:

$$\tilde{u}_{111} = \frac{i}{D}\frac{\hat{k}_1}{Vk}\left[-{c_{44}}^2\hat{k}_1^2 + c_{11}c_{44}\left(2\hat{k}_2^2\hat{k}_3^2 - \hat{k}_2^2 - \hat{k}_3^2\right) + \left({c_{12}}^2 + 2c_{12}c_{44} - {c_{11}}^2\right)\hat{k}_2^2\hat{k}_3^2\right]$$

$$\tilde{u}_{211} = \frac{i}{D}\frac{\hat{k}_1^2\hat{k}_2}{Vk}\left[(c_{12}+c_{44})\left(c_{44} + (c_{11}-c_{12}-2c_{44})\hat{k}_3^2\right)\right]$$

$$\tilde{u}_{112} = \frac{i}{D}\frac{\hat{k}_2}{2Vk}\left[-c_{11}c_{44}\left(\hat{k}_1^2\hat{k}_2^2 + \hat{k}_2^4 + \hat{k}_3^4\right) + c_{12}c_{44}\left(\hat{k}_1^4 + \hat{k}_1^2\hat{k}_2^2 - 2\hat{k}_1^2\hat{k}_3^2 + 2\hat{k}_2^2\hat{k}_3^2\right) - {c_{11}}^2\hat{k}_2^2\hat{k}_3^2 + {c_{12}}^2\left(\hat{k}_2^2\hat{k}_3^2 - \hat{k}_1^2\hat{k}_3^2\right) - 2{c_{44}}^2\hat{k}_1^2\hat{k}_3^2 + c_{11}c_{12}\hat{k}_1^2\hat{k}_3^2\right]$$

$$\tilde{u}_{312} = \frac{i}{D}\frac{\hat{k}_1\hat{k}_2\hat{k}_3}{2Vk}\left[(c_{12}+c_{44})\left(\left(c_{11}-c_{12}\right)\left(\hat{k}_1^2+\hat{k}_2^2\right) + 2c_{44}\hat{k}_3^2\right)\right]. \tag{69}$$

The other components of $\tilde{u}$ are related to those above by cubic symmetry. These equations reduce to equation (62) if we set the elastic constants to their isotropic values, that is, $c_{11} \to \lambda + 2\mu$, $c_{12} \to \lambda$, and $c_{44} \to \mu$.

Then the $\tilde{\epsilon}_{ijkl}$ are given by equation (38). As can be verified from the above formulas, $\tilde{\epsilon}_{ijkl}$ is symmetric under interchange of ij and kl, as it was in the isotropic case.

however, that for moderate values of u_M the polynomial cutoffs seem to work better. The bump integrals usually give wild oscillations at small values of u_M before getting into the exponential regime, while the polynomials behave better at small u_M. In the examples shown, at $u_M = 100$, or after about 16 cycles of $\sin(u)$, the two methods are giving about the same accuracy. At smaller values of u_M, the polynomial cutoff does much better.

For the elasticity problem, in summing over Fourier modes in three dimensional space, the computer time grows like ${u_M}^3$, and we generally are able to sum over wave vectors about 10 times as big as the wave vector corresponding to shortest separation between dipoles. We have used the P_8 for the cutoff functions for the work in this thesis.

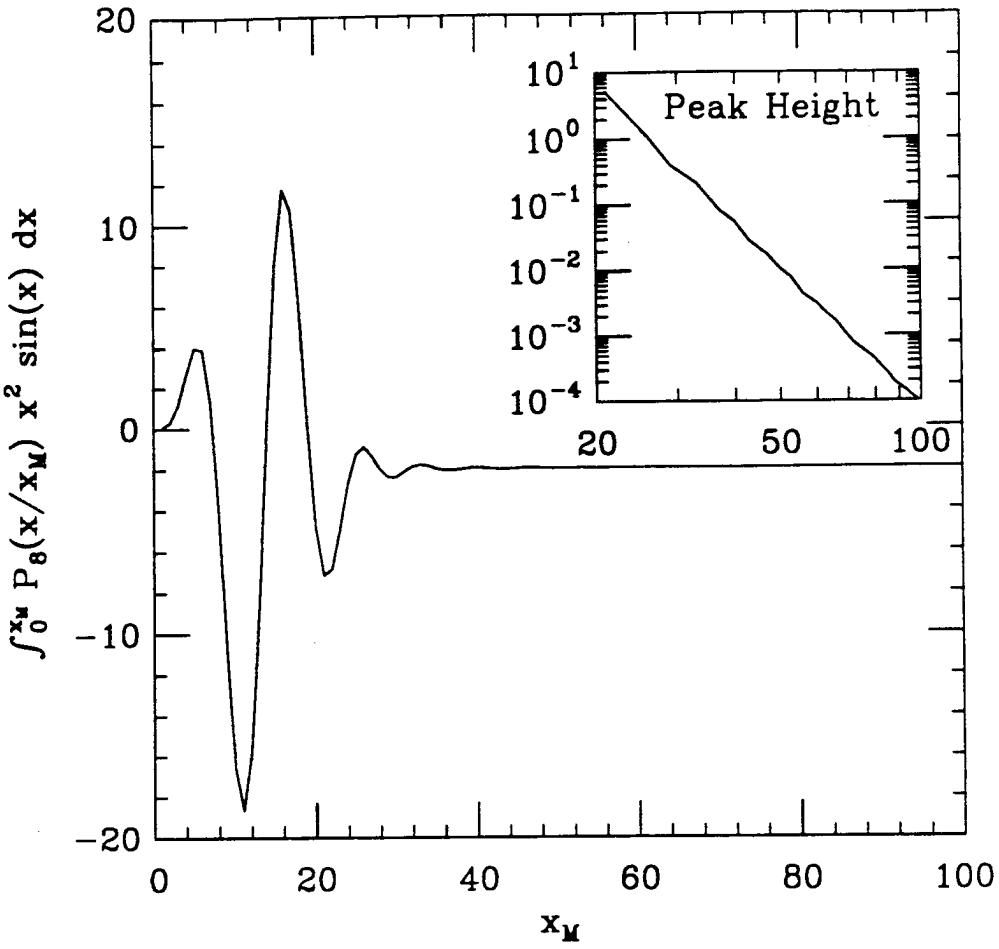

Figure 3.1 This shows a graph of $\int_0^x f(u/x)u^2 sin(u)du$ where f(u) is $P_8(u)$, given in Table 1. The inset is a graph of the peak height as a function of x, plotted on a log-log scale. We see that the peak height is decaying with a power law, where the power is close to -7, as expected.

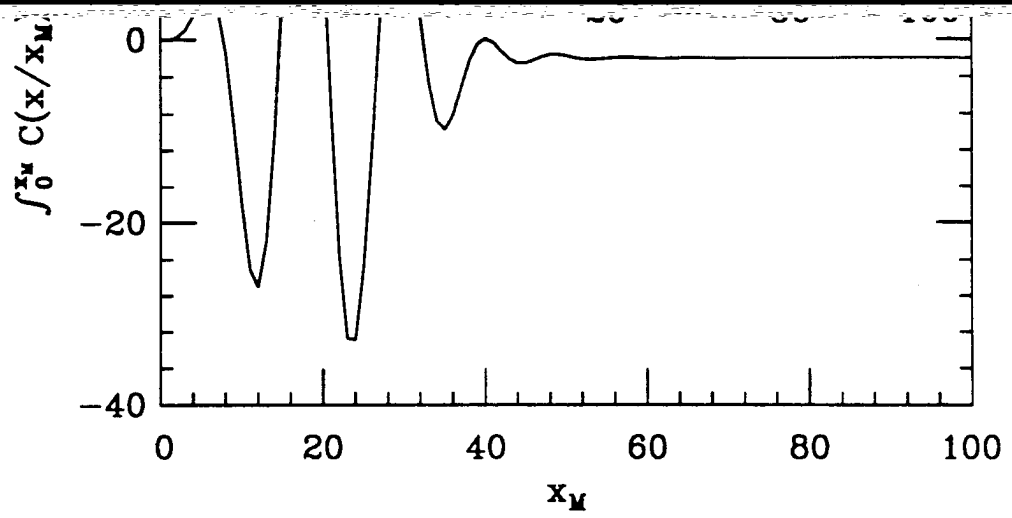

Figure 3.2 This contains a graph of $\int_0^x f(u/x)u^2 sin(u)du$ where f(u) is the integral of the bump function for parameters a=0.0 and b=0.05. The inset is a graph of the peak height as a function of x, plotted on a semi-log scale. We see that the peak height is decaying exponentially.

experiments, and we will be able to compare the distributions that we measure with the experimental distributions. We do this in chapter 6.

Another reason that barrier heights are of interest is that there have been two recent theoretical calculations of distributions of barrier heights in quadrupolar glasses. The two groups analyzed somewhat different models, both of which simplify the actual elastic dipole interaction, and which embody different aspects of the physics present in this system. Sethna and Chow[13,14,15] have calculated a mean field theory for a model which ignored the frustration of the elastic dipole interaction, but included the effect of dilution, the fact that different dipoles have different numbers of near neighbors. Kanter and Sompolinsky[16] have performed a mean field theory of a model which is frustrated, but in which all the dipoles are equivalent, each dipole interacts with all the other dipoles.

There are two barriers heights which we will calculate in the next two sections. The *bare* barrier is the barrier to the reorientation of a particular dipole when all the other dipoles are fixed. This is given by Q_0 times the difference between the largest two eigenvalues of the strain tensor evaluated at the dipole. This is the barrier height calculated in the theoretical calculations, so we will compare this barrier to the theories.

The bare barrier is actually an upper limit to the physical barrier height, since in the real world, the other dipoles will relax as one dipole flips over. If the process is thermally activated, as the distribution measured experimentally in KBr:KCN is, the barrier important for the reorientation rate of a dipole will be given by the lowest energy saddle that the system has to go through as one dipole reorients itself. We therefore also calculate a *relaxed* barrier height, where we allow the other dipoles to adjust as a given dipole flips over. In the next two

the dipoles, and since we place the dipoles on a lattice, many pairs of dipoles will be separated by the same displacement vector and therefore have the same J_{ijkl}. Similarly, the J_{ijkl} values even for different displacement vectors will not

4.5 Simulation with Cubic Elastic Constants

We have also run the simulation using cubic elastic constants, partly in hopes that we would get the correct ground state for KCN when we put dipoles on all of the sites. KCN at low temperatures has an orthorhombic structure, with the long axes of the cyanides pointing in a direction corresponding to a $\langle 110 \rangle$ direction in a cubic lattice. Using the elastic constants for KBr as our bare elastic constants, however, it turns out that the pure system prefers the same state as the isotropic case, that is, the Pa3 state. Among the ferroelastic states, that is states with the dipoles all pointing in the same direction, the best one is not even the $\langle 110 \rangle$ state, but the $\langle 111 \rangle$ state.

CHAPTER V — HARMONIC STUFF

5.1 Introduction

In this chapter we will discuss properties of the harmonic excitations about the ground state.

We will be considering the orientational (which we will call librational) normal modes of the dipoles, treating them separately from the phonon modes. We will include the effects of the phonons in a perturbative fashion. Actually, since the interactions between the dipoles are mediated by the phonons, the true normal modes of the system involve both the librational and phonon degrees of freedom. In treating the phonons and libration modes separately, we are making an approximation based on a separation of time scales. If the frequencies of the

Substituting (143) into the formula for the interaction energy gives

$$-\sum_b \frac{C_{b,ij}(\mathbf{k})C_{b,kl}(\mathbf{k})}{I}\chi(\omega;\Omega_b)\epsilon^E_{ij}\epsilon^E_{kl}. \tag{147}$$

Comparing this to $V\delta s_{ijkl}\sigma^E_{ij}\sigma^E_{kl}$, we obtain the change in the compliance tensor of the medium due to the phonon–libration coupling,

$$\delta s_{ijkl}(\omega) = -\frac{s_{iji'j'}s_{klk'l'}}{IV}\sum_b C_{b,i'j'}C_{b,k'l'}\chi(\omega;\Omega_b) \tag{148}$$

Since the susceptibility is complex, the change in the compliance tensor has a part which is in phase with the external perturbation and one that is out of phase. We shall show below that, in the usual way, the real (in-phase) part represents a change in the elastic constants of the medium and the imaginary (out-of-phase) part, a lifetime for the phonon excitations.

Before proceeding to the final physical results, we need to simplify (148) into a more manageable form. We will first perform a spherical average over the libration modes in the system. With the one additional assumption that the relevant phonon wavelength $2\pi/k$ is much larger than the (assumed) localization length of the libration modes, the angular average $\langle C_{b,ij}(\mathbf{k})C_{b,kl}(\mathbf{k})\rangle$ may be evaluated in much the same way as in the static case. We use this to obtain the same result as before, namely

$$\langle C_{b,ij}C_{b,kl}\rangle\frac{Q_0^2A_b^2}{15}\Big[-2\delta_{ij}\delta_{kl}+3(\delta_{ik}\delta_{jl}+\delta_{il}\delta_{jk})\Big], \tag{149}$$

the phonon wave vector having disappeared from this result since we have effectively taken the $k \to 0$ limit.

Next we denote the average over the libration modes in (148) by a sum over the distribution of libration frequencies via the replacement $\frac{1}{V}\sum_b \to \int d\Omega p(\Omega)$.

and

$$B''(\omega) = \frac{\Upsilon}{\mu} \int d\Omega p(\Omega) A^2(\Omega) \frac{\omega \Gamma(\omega)}{\left(\Omega^2 - \omega^2\right)^2 + \omega^2 \Gamma^2(\omega)}. \tag{152}$$

Finally, using equation (125) which gives the compliance tensor in terms of the Lamé coefficients, together with (149) we find that the change in the compliance tensor, equation (148), spherically averaged, reduces to

$$\delta s_{ijkl} = \frac{B(\omega)}{60\mu} \left[-2\delta_{ij}\delta_{kl} + 3\left(\delta_{ik}\delta_{jl} + \delta_{il}\delta_{jk}\right) \right] \tag{153}$$

with $B(\omega)$ given by (150). Note that in the static limit ($\omega = 0$), we recover our earlier result.

5.4.2 Frequency Dependent Elastic Constants

We will now focus on the real and imaginary parts of (153). We will find it convenient to first work out the longitudinal (L) and transverse (T) components of the compliance tensor. For a general tensor with the symmetries of s_{ijkl}

$$A_{ijkl} = B\delta_{ij}\delta_{kl} + C\left(\delta_{ik}\delta_{jl} + \delta_{il}\delta_{jk}\right) \tag{154}$$

these are given by

$$A^{(L)} = B + 2C \qquad \text{and} \qquad A^{(T)} = C, \tag{155}$$

details of the distribution than the thermal conductivity. This is because, while the plateau in the thermal conductivity is caused by the majority of modes in the center of the distribution, the specific heat bump is caused by the low tail of the distribution. A bump happens because the density of states starts growing faster than ω^2, but soon grows slower than ω^2.

The large bump seen in the $x = 0.7$ simulation is actually due to the phonons. Since we determined the bare elastic constants from $x = 0.5$, the simulation's prediction of the soft speed of sound for $x = 0.7$ does not have to fit the experimental value, and in fact it doesn't. In the simulation at $x = 0.7$, there are some low frequency modes that couple extremely strongly to the phonons, and these lead to a large softening, the predicted low frequency (1.3×10^5 cm/sec) is quite a bit less than the experimental value (1.6×10^5 cm/sec). This difference may have

libration modes. We ignore the time–retarded nature of the interaction in calculating the frequencies of the libration modes, but this appears to be an excellent approximation: the interaction energy is dominated by neighbors within a couple of lattice constants (high–frequency phonons).

We share with Yu and Leggett a dissatisfaction with the traditional tunneling center approaches. We believe, however, that quantum tunneling is probably necessary to get the very long time scales and the large density of states at low energies. Low energy excitations at long wavelengths should be suppressed by phase space; also, they ought to contribute to thermal transport (which experimentally is dominated by phonons[38]). The only ways we can see to have localized low energy excitations involve tunneling through barriers. We believe also that more or less localized harmonic excitations are probably responsible for the plateau and the anomalous specific heat at intermediate temperatures in glasses.

7.2 Conclusions

A large part of the reason for the fairly rapid acceptance of the TLS model as a paradigm in glasses was that it correctly predicted new features, such as saturable acoustic absorption. Are there any testable consequences of our model? One prediction involves the softening seen in glasses. The speed of sound in amorphous materials is typically less than that in crystalline forms of the same material. In our model this is due to the same excitations that lead to the plateau in the thermal conductivity. We therefore predict that at frequencies of 10 Terahertz or so, glassy materials should become stiffer. We realize, of course, that this is a rather high frequency.

Another prediction of our model is that glasses should possess localized harmonic modes. Resonant scattering from these modes leads to the plateau. We have mentioned in chapter 6 the excess low frequency modes seen by Buchenau *et al.* in vitreous silica. In general it may be difficult to see these modes experimentally, but they should also appear in computer simulations of glasses. In a

by

$$B = \frac{8x}{\tilde{\mu}} \int d\tilde{\Omega}\, \frac{\tilde{p}(\tilde{\Omega})\overline{A^2}}{\tilde{\Omega}^2}. \tag{200}$$

Using equation (162) for the mean speed of sound in an isotropic material, and (132) for the softened elastic constants, we get the low frequency Debye velocity to be

$$v_D = \sqrt{\frac{\gamma\tilde{\mu}}{\rho\left(1+\frac{B}{5}\right)}} \left[\frac{3}{2+\left(\frac{\tilde{\mu}}{\tilde{\lambda}+2\tilde{\mu}+\frac{B}{5}\left(\frac{2}{3}\tilde{\mu}+\tilde{\lambda}\right)}\right)^{3/2}}\right]^{\frac{1}{3}}. \tag{201}$$

This gives

$$\gamma = \frac{v_D^2\rho\left(1+\frac{B}{5}\right)}{\tilde{\mu}} \left[\frac{2}{3}+\frac{1}{3}\left(\frac{\tilde{\mu}}{\tilde{\lambda}+2\tilde{\mu}+\frac{B}{5}\left(\frac{2}{3}\tilde{\mu}+\tilde{\lambda}\right)}\right)^{3/2}\right]^{\frac{2}{3}}. \tag{202}$$

Now we know γ in terms of the measured Debye velocity and the inputs to the simulation, x, $\tilde{\mu}$, and $\tilde{\lambda}$. As we have mentioned before, only the ratio of $\tilde{\mu}$ and $\tilde{\lambda}$ is important, if we double $\tilde{\mu}$ and $\tilde{\lambda}$, this lowers the computer's energy scale, so that B also doubles, and finally γ will end up being halved, giving the same high frequency values for μ and λ, as desired. Now that we know the "bare" values of μ and λ, we know everything we need to know, since we will take Υ and y from experiment.

APPENDIX C – ISOTROPIC MINIMUM ENERGY CONFIGURATION

In this appendix we determine the minimum energy arrangement of two dipoles in an infinite isotropic medium. We take the line connecting them to be the z axis, and indicate the directions of the dipoles by angular coordinates (θ, ϕ) and (α, β). We can take $\beta = 0$ without loss of generality. The interaction energy of a configuration is given by $E = -J_{ijkl} Q_{ij}(\alpha, 0) Q_{kl}(\theta, \phi)$, where the J_{ijkl} are given in section XXX, eq. (22). For dipoles in the z direction from each other, the nonzero components of J_{ijkl} are

$$\begin{aligned} J_{1111} = J_{2222} &= A[4 - 6B] \\ J_{3333} &= -8A \\ J_{1122} &= -2AB \\ J_{1133} = J_{2233} &= 4AB \\ J_{1212} &= A[2 - 2B] \\ J_{1313} = J_{2323} &= A[-1 + 4B], \end{aligned} \tag{203}$$

where

$$A = \frac{1}{16\pi\mu z^3} \qquad \text{and} \qquad B = \left(\frac{\lambda+\mu}{\lambda+2\mu}\right). \tag{204}$$

In the following we will have to constrain the possible values of B. The condition for an isotropic medium to be thermodynamically stable is that both the shear modulus μ and the bulk modulus $K = \lambda + \frac{2}{3}\mu$ must be greater than zero. This implies that

$$\frac{1}{4} < B < 1. \tag{205}$$

We will take A to be equal to one, since it is just determines the scale of the energy. We now consider separately the contributions to the energy given by the

terms in J_{ijkl} which are independent of B, and the parts which depend on B. We will call these two terms E_1 and E_2 respectively.

Using (203), and writing out the Q_{ij}'s as a function of θ, ϕ, and α, we get that the part of the energy which doesn't depend on B is equal to

$$E_1 = 2\left[\frac{4}{3} - 2\cos^2\alpha\sin^2\theta - 2\sin^2\alpha\cos^2\theta - 2\sin^2\alpha\sin^2\theta\cos^2\phi + 2\cos\alpha\sin\alpha\cos\theta\sin\theta\cos\phi\right]. \tag{206}$$

The minimum value for this term is $-11/6$, which occurs at $\theta = \alpha = \frac{\pi}{3}$, and $\phi = \pi$. In this state the dipoles are coplanar, and their directors form an "X", with the lines of the X at 60°to the z axis.

The part of the energy which depends on B is given by

$$E_2 = 2B\left[\frac{8}{3} + 5\sin^2\alpha\sin^2\theta - 4\sin^2\alpha - 4\sin^2\theta + 2\sin^2\alpha\sin^2\theta\cos^2\phi - 8\cos\alpha\sin\alpha\cos\theta\sin\theta\cos\phi\right]. \tag{207}$$

The minimum value for this term is $-16/5B$. This occurs when θ and α are both equal to $\arcsin\sqrt{32/60} \approx 0.818$, and $\phi = 0$. In this state the dipoles are parallel to each other, and tilted with respect to the z axis.

It is easy to show that in the minimum energy state we must have $\cos^2\phi = 1$. To do this, we note that the part of the interaction energy which depends on ϕ is

$$4\sin^2\alpha\sin^2\theta\cos^2\phi\,(B-1) + 4\cos\alpha\sin\alpha\cos\theta\sin\theta\cos\phi\,(-4B+1). \tag{208}$$

The second term can be either positive or negative, so its minimum occurs when either $\cos\phi = 1$ or -1. Since the first term is always negative, it is also minimized when $\cos^2\phi = 1$.

Actually, neither of the states we have mentioned is the minimum energy state. A compromise between the two states is the "Tee" state, in which $\alpha = \frac{\pi}{2}$ and $\theta = 0$. In this state the dipoles form a Tee, with one dipole perpendicular and one parallel to the line connecting them. The total interaction energy for the states which we have discussed are, for the T state, $-4/3 - 8/3B$; for the X state, $-11/6 + 101/24B$; and for the parallel state, $8/15 - 16/5B$. So for thermodynamically stable values of B, the T state always wins over these states.

Expanding the energy in θ and α about the T state gives

$$E \approx -4/3 - 8/3B + 2\theta^2\left(2 + B + 2\cos^2\phi\,(B-1)\right) + 4\delta^2(1+2B) + 4\theta\delta\,(4B-1)\cos\phi, \tag{209}$$

where $\delta \equiv \alpha - \frac{\pi}{2}$. For the T state to be stable, this must have a minimum at $\theta = \delta = 0$. Recall that for $ax^2 + by^2 + cxy$ to have a minimum at zero, it is required that $4ab > c^2$. Here we need to show that

$$\left(2+4B\right)\left(2+B+2\cos^2\phi\,(B-1)\right) \;>\; \left(1-8B+16B^2\right)\cos^2\phi. \tag{210}$$

Setting $\cos^2\phi = 1$, we get

$$\left(6B+12B^2\right) \;>\; \left(1-8B+16B^2\right), \tag{210}$$

which is true for $\frac{1}{4} < B < 1$.

So the T state is a local minimum. I have verified numerically that it is also a global minimum, by plotting the energy as a function of θ and ϕ. There are clearly no other competitive states in total energy, and I don't think that there are even any metastable states for the acceptable values of B.

APPENDIX D – HARMONIC SUSCEPTIBILITY

In this appendix we will derive the susceptibility of a libration mode to the phonon strain fields. Most of the discussion of the results this section occur in section 5.4.1.

We want to calculate the susceptibility to a given phonon strain field of a "tagged" libration mode coupled to the bath of all the other phonons. We first do this in a general context[43]. Consider a harmonic oscillator with coordinate X driven by an external force F, and coupled to a bath of harmonic oscillators with coordinates x_k. The coupling is linear in both oscillator coordinates, with strength c_k. The Hamiltonian of the whole system is given by

$$H = \frac{P^2}{2M} + \frac{1}{2}M\Omega^2 X^2 - FX + \sum_k (\frac{p_k^2}{2m_k} + \frac{1}{2}m_k\omega_k^2 x_k^2) + \sum_k c_k x_k X. \qquad (211)$$

The equations of motion for X and x_k are:

$$M\ddot{X} + M\Omega^2 X + \sum_k c_k x_k = F \qquad (212)$$

$$m_k\ddot{x}_k + m_k w_k^2 x_k + c_k X = 0. \qquad (213)$$

We take the Fourier Transform of eq. (213), using the convention

$$x_k(t) = \int \tilde{x}_k(\omega) e^{i\omega t}\frac{d\omega}{2\pi} \qquad \tilde{x}_k(\omega) = \int x_k(t) e^{-i\omega t} d\omega. \qquad (214)$$

This gives

$$\tilde{x}_k = \frac{c_k}{m_k(\omega^2 - \omega_k^2)}\tilde{X}. \qquad (215)$$

We can eliminate the $\tilde{x}_k$ in the Fourier Transform of eq. (212) to get

$$M(\Omega^2 - \omega^2)\tilde{X} + \sum_k \frac{c_k^2}{m_k(\omega^2 - \omega_k^2)}\tilde{X} = \tilde{F}. \qquad (216)$$

Defining the susceptibility χ by

$$\tilde{X}(\omega) = \frac{\chi(\omega)}{M}\tilde{F}(\omega) \tag{217}$$

we get

$$\chi(\omega) = \left[(\Omega^2 - \omega^2) + \frac{1}{M}\sum_k \frac{c_k^2}{m_k(\omega^2 - \omega_k^2)}\right]^{-1}. \tag{218}$$

In the limit of a phonon bath with a large number of degrees of freedom, the sum over k becomes an integral over a phonon density of states, $g(\omega)$,

$$\frac{1}{V}\sum_k \longrightarrow \int d\omega_k\, g(\omega_k). \tag{219}$$

To make the integral over t in (214) well defined for $\omega > 0$, we let $\omega \to w - i\eta$, $\eta = 0+$. Then

$$\frac{1}{M}\sum_k \frac{c_k^2}{m_k(\omega^2 - \omega_k^2)} = \frac{V}{M}\int_0^\infty d\omega_k\, g(\omega_k)\frac{c_k^2}{m_k(\omega + \omega_k)(\omega - i\eta - \omega_k)} \tag{220}$$

$$= \frac{V}{M}\ \mathrm{P}\int_0^\infty d\omega_k\, g(\omega_k)\frac{c_k^2}{m_k(\omega^2 - \omega_k^2)} + \frac{i\pi V}{M}\int_0^\infty d\omega_k\, g(\omega_k)\frac{c_k^2}{m_k(\omega + \omega_k)}\delta(\omega - \omega_k) \tag{221}$$

$$= \Delta(\omega) + i\omega\Gamma(\omega), \tag{222}$$

where

$$\Delta(\omega) \equiv \frac{V}{M}\ \mathrm{P}\int_0^\infty d\omega_k\, g(\omega_k)\frac{c_k^2}{m_k(\omega^2 - \omega_k^2)} \tag{223}$$

$$\Gamma(\omega) \equiv \frac{\pi V g(\omega)c_k^2(\omega)}{2Mm(\omega)\omega^2}. \tag{224}$$

The susceptibility is then given by

$$\chi(\omega) = \left[(\Omega^2 - \omega^2) + \Delta(\omega) + i\omega\Gamma(\omega)\right]^{-1} \equiv \chi'(\omega) - i\chi''(\omega). \tag{225}$$

We now go to the specific case of interest, that is a libration mode coupled to a bath of phonons. We consider a single libration mode of frequency Ω_b, coupled to all the phonon modes, one of which is considered to be driving the libration mode. We calculate the susceptibility of the libration mode to the strain field of the special phonon mode, defining the susceptibility by

$$\psi_b(\omega) = -\frac{C_{b,ij}}{I}\chi(\omega;\Omega_b)\epsilon^E_{ij}. \tag{226}$$

The strain field of a phonon with amplitude ϵ_0 and polarization $\hat{\eta}$ is

$$\epsilon_{ij}(\mathbf{k},\hat{\eta}) = \frac{1}{2}\left(\hat{\eta}_i k_j + \hat{\eta}_j k_i\right)\epsilon_0(\mathbf{k},\hat{\eta})e^{i(\mathbf{k}\cdot\mathbf{x}-\omega t)}. \tag{227}$$

Now, for the case of libration modes and phonons, eq. (211) becomes

$$\begin{aligned} H = \frac{L^2}{2I} + \frac{1}{2}I\Omega_b^2\psi_b^2 - C_{b,kl}(\mathbf{k})\psi_b\epsilon^E_{kl}(\mathbf{k},\eta) \\ + \sum_{\mathbf{k},\hat{\eta}}\left(\frac{p_k^2}{2\rho V} + \frac{1}{2}\rho V\omega_k^2\epsilon_0^2\right) - \sum_{\mathbf{k},\hat{\eta}} C_{b,ij}(\mathbf{k})\psi_b\epsilon_{ij}(\mathbf{k},\eta), \end{aligned} \tag{228}$$

from equation (140). The forcing is due to the phonon considered to be driving the libration mode, which we have labeled with a superscript E. As before, we take the Fourier transform of the equation of motion for the ϵ_0's giving

$$\tilde{\epsilon}_0(\mathbf{k},\hat{\eta}) = \frac{\frac{1}{2}C_{b,ij}(\hat{\eta}_i k_j + \hat{\eta}_j k_i)}{\rho V\left(\omega^2 - \omega_k^2\right)}\tilde{\psi}_b \tag{229}$$

Putting this into the equation for ψ_b gives

$$I\left(\Omega_b^2 - \omega^2\right)\tilde{\psi}_b + \sum_{\mathbf{k},\hat{\eta}}\frac{\frac{1}{4}C_{b,ij}(\hat{\eta}_i k_j + \hat{\eta}_j k_i)C_{b,kl}(\hat{\eta}_k k_l + \hat{\eta}_l k_k)}{\rho V\left(\omega^2 - \omega_k^2\right)}\tilde{\psi}_b = C_{b,ij}\tilde{\epsilon}^E_{ij} \tag{230}$$

We now wish to average this formula over orientations of the libration modes. We will consider longitudinal (L) and transverse (T) phonons separately. Assuming that the spatial extent of the libration mode is much smaller than the

wavelength of the phonon, we can perform the spherical average in the same way as we did for the static case in section 5.3. We will define the longitudinal and transverse parts of $\langle C_{b,ij}C_{b,kl}\rangle$ so that

$$\langle C_b^2\rangle^{(\eta)}\left(\epsilon^{(\eta)}\right)^2 = \langle C_{b,ij}C_{b,kl}\rangle\ \epsilon_{ij}\epsilon_{kl} \tag{231}$$

From section 5.3 we know that

$$\langle C_{b,ij}C_{b,kl}\rangle = \frac{Q_0^2A_b^2}{15}\Big[-2\delta_{ij}\delta_{kl} + 3(\delta_{ik}\delta_{jl} + \delta_{il}\delta_{jk})\Big], \tag{232}$$

so it can be seen that

$$\langle C_b^2\rangle^{(L)} = \frac{4Q_0^2A_b^2}{15} \tag{233}$$

$$\langle C_b^2\rangle^{(T)} = \frac{Q_0^2A_b^2}{5} \tag{234}.$$

The sum over $\mathbf{k}$ and $\hat{\eta}$ then becomes a sum over the longitudinal and transverse phonons. Now equation (230) becomes

$$I\left(\Omega_b^2 - \omega^2\right)\tilde{\psi}_b + \left[\frac{4}{15}\sum_{\mathbf{k}}\frac{Q_0^2A_b^2k^2}{\rho V\left(\omega^2 - \omega_{kL}^2\right)} + \frac{2}{5}\sum_{\mathbf{k}}\frac{Q_0^2A_b^2k^2}{\rho V\left(\omega^2 - \omega_{kT}^2\right)}\right]\tilde{\psi}_b = C_{b,ij}\tilde{\epsilon}_{ij}^E, \tag{235}$$

and the susceptibility then becomes

$$\chi(\omega;\Omega_b) = \left[\left(\Omega_b^2 - \omega^2\right) + \frac{4}{15}\sum_{\mathbf{k}}\frac{Q_0^2A_b^2k^2}{I\rho V\left(\omega^2 - \omega_{kL}^2\right)} + \frac{2}{5}\sum_{\mathbf{k}}\frac{Q_0^2A_b^2k^2}{I\rho V\left(\omega^2 - \omega_{kT}^2\right)}\right]^{-1} \tag{236}$$

Following the derivation of equations (224) and (225) we get

$$\Delta(\omega) = \frac{4}{15}\frac{\Upsilon A_b^2}{\rho}\,P\int d\omega_k\frac{g_L(\omega_k)k_L^2(\omega)}{\left(\omega^2 - \omega_k^2\right)} + \frac{2}{5}\frac{\Upsilon A_b^2}{\rho}\,P\int d\omega_k\frac{g_T(\omega_k)k_T^2(\omega)}{\left(\omega^2 - \omega_k^2\right)} \tag{237}$$

$$\Gamma(\omega) = \frac{4\pi g_L(\omega)Q_0^2A_b^2k_L^2(\omega)}{30I\rho\omega^2} + \frac{2\pi g_T(\omega)Q_0^2A_b^2k_T^2(\omega)}{10I\rho\omega^2}, \tag{238}$$

where, as in section 5.3, $\Upsilon \equiv Q_0^2/I$.

Finally, if we take the phonon density of states for each polarization to be given by a Debye distribution, $g(\omega) = \omega^2/2\pi^2 v^3$, then we get

$$\Delta(\omega) = \frac{2}{15}\frac{\Upsilon A_b^2}{\rho} P\int d\omega_k \frac{\omega^4}{\pi^2 v_L^5 \left(\omega^2 - \omega_k^2\right)} + \frac{1}{5}\frac{\Upsilon A_b^2}{\rho} P\int d\omega_k \frac{\omega^4}{\pi^2 v_T^5 \left(\omega^2 - \omega_k^2\right)} \quad (239)$$

$$\Gamma(\omega) = \left(\frac{2}{3v_L^5} + \frac{1}{v_T^5}\right)\frac{\Upsilon A_b^2 \omega^2}{10\pi\rho}. \quad (240)$$

The real part of the above expression, $\Delta(\omega)$ can be interpreted as a shift in the frequency Ω_b of the libration mode due to a renormalization of the moment of inertia I.

We write the susceptibility as

$$\chi(\omega;\Omega_b) = \chi'(\omega;\Omega_b) - i\chi''(\omega;\Omega_b). \quad (241)$$

Expressing the libration frequency in terms of the renormalized frequency, the real and imaginary parts of $\chi(\omega;\Omega_b)$ are given by

$$\chi'(\omega;\Omega_b) = \frac{\Omega_b^2 - \omega^2}{\left(\Omega_b^2 - \omega^2\right) + \omega^2\Gamma^2(\omega)} \quad (242)$$

$$\chi''(\omega;\Omega_b) = \frac{\omega\Gamma(\omega)}{\left(\Omega_b^2 - \omega^2\right) + \omega^2\Gamma^2(\omega)} \quad (243)$$

We now return you to section 5.4.1.

REFERENCES

1. J.M. Ziman, *Electrons and Phonons: The Theory of Transport Phenomena in Solids*, (Oxford, London, 1960).

2. R.C. Zeller and R.O. Pohl, Thermal Conductivity and Specific Heat of Noncrystalline Solids, *Phys. Rev. B* **4**, 2029 (1971).

3. P. W. Anderson, B. I. Halperin, and C. M. Varma, *Phil. Mag.* **25**, 1 (1972).

4. W. A. Phillips, *J. Low Temp. Phys.* **7**, 351 (1972).

5. W.A. Phillips in *Amorphous Solids, Low Temperature Properties*, edited by W.A. Phillips, (Springer–Verlag, Berlin, 1981).

6. U. Buchenau, M. Prager, N. Nucker, A. J. Dianoux, N. Ahmad, W. A. Phillips, *Phys. Rev. B* **34**, 5665 (1986).

7. U. Buchenau, H. M. Zhou, N. Nucker, K. S. Gilroy, W. A. Phillips, *Phys. Rev. Lett.* **60**, 1318 (1988).

8. A.E.H. Love, *The Mathematical Theory of Elasticity*, (Cambridge University Press, Cambridge, 1927).

9. L.D. Landau and E.M. Lifshitz, *Theory of Elasticity*, (Pergamon, New York, 1959).

10. J. P. Hirth and J. Lothe, *Theory of Dislocations*, (Wiley, New York, 1982).

11. I.M. Lifshitz and L.N. Rozenzweig, Green's tensor for anisotropic unbounded elastic medium, *Zh. Eksper. Teor. Fiz.* **17**, 783 (1947).

12. J. D. Eshelby, *Solid State Phys.* **3**, 79 (1956).

13. J. P. Sethna and K. S. Chow, *Phase Trans.* **5**, 317 (1985).

14. J. P. Sethna, *Annals of the NYAS* **484**, 130 (1986).

15. M. Meissner, W. Knaak, J.P. Sethna, K.S. Chow, J.J. DeYoreo, and R.O. Pohl, *Phys. Rev. B* **32**, 6091 (1985).

16. I. Kanter and H. Sompolinsky *Phys. Rev. B* **33**, 2073 (1986).

17. C.I. Nicholls, L.N. Yadon, D.G. Haase, and M.S. Conradi, *Phys. Rev. Lett.* **59**, 1317 (1987).

18. J.J. De Yoreo, W. Knaak, M. Meissner, and R.O. Pohl, *Phys. Rev. B* **34**, 8828 (1986) and references therein.

19. O.L. Anderson, *J. Phys. Chem. Solids* **12**, 41 (1959).

20. Using the shape factor and rotational constant measured by H. Beyeler, *Phys. Rev. B* **11**, 3078 (1975), we arrive at values $Q_0 = 1.1$eV and $I = 2.8 \times 10^{-39}$g-cm^2 respectively. This gives a value for Υ of 1.1×10^{15} erg/sec^2. While we use this value, note that the uncertainty in these quantities is rather large; R. Spitzer (Ph.D. Thesis, Cornell University, (1987)), estimates $I = 6.5 \times 10^{-39}$g-cm^2.

21. A.M. de Goër, in *Phonon Scattering in Condensed Matter V*, ed. A.C. Anderson and J.P. Wolfe, (Springer–Verlag, Berlin, 1986).

22. M. Randeria and J.P. Sethna, *Phys. Rev. B* **38**, 12607 (1988); M. Randeria, Ph.D. Thesis, Cornell University, (1987), (unpublished).

23. H.U. Beyeler, *Phys. Rev. B* **11**, 3078 (1975).

24. F. Luty, in *Defects in Insulating Crystals*, edited by V. M. Turkevich and K. K. Swartz (Springer Verlag, Berlin, 1982), p. 69.

25. Find this out

26. C. C. Yu and J. J. Freeman, *Phys. Rev. B* **36**, 7850 (1987). Yu and Freeman achieve a good fit to the date by including a large amount of Rayleigh scattering. As noted above, we find that Rayleigh scattering is not an important until above the plateau region.

27. J. E. Graebner, B. Golding, and L. C. Allen, *Phys. Rev. B* **34**, 5696 (1986).

28. S. Hunklinger and W. Arnold, in *Physical Acoustics*, Vol. 12, ed. R.N. Thurston and W.P. Mason, (Academic, N.Y., 1976).

29. S.K. Watson, D.G. Cahill, and R.O. Pohl, submitted to Physical Review B.

30. N.O. Birge, Y.H. Jeong, S.R. Nagel, S. Bhattacharya, and S. Susman, *Phys. Rev. B* **30**, 2306 (1984).

31. L. Wu, R.M. Ernst, Y.H. Jeong, S.R. Nagel, and S. Susman, *Phys. Rev. B* **10444**, 37 (1988).

32. C. M. Varma, R. C. Dynes, and J. R. Banavar, *J. Phys. C.* **15**, 1221 (1982).

33. M. W. Klein, *Phys. Rev. B* **29**, 5825 (1982).

34. S. Alexander *et al.*, *Phys. Rev. B* **28**, 4615 (1983), and S. Alexander, O. Entin-Wohlman, and R. Orbach, *Phys. Rev. B* **34**, 2726 (1986).

35. V. G. Karpov and D. A. Parshin, *Sov. Phys. JETP* **61**, 1308 (1985) (*Zh. Eksp. Teor. Fiz.* **88**, 2212 (1985)).

36. C. C. Yu and A. J. Leggett, submitted to Comments on Condensed Matter Physics.

37. M.P. Zaitlin and A.C. Anderson, *Phys. Rev. B* **12**, 4475 (1975).

38. R. Biswas, A.M. Bouchard, W.A. Kamitakahara, G.S. Grest, and C.M.Soukoulis, *Phys. Rev. Lett.* **60**, 2280 (1988).

39. P.B. Allen and J.L. Feldman, submitted to Physical Review Letters.

40. S.A. Langer and J.P. Sethna, *Phys. Rev. Lett.* **61**, 570 (1988).

41. The rejection method is discussed in *Numerical Recipes*, by W. H. Press, B. P. Flannery, S. A. Teukolsky, and W. T. Vetterling (Cambridge, Cambridge, 1986), p. 203.

42. D.L. Huber and J.H. Van Vleck, *Rev. Mod. Phys.* **38**, 187 (1966).

43. Recent remeasurements of the cyanide concentrations (reference 29) of the $KBr_{(1-x)}KCN_x$ samples used by De Yoreo *et al.* indicate that the actual concentrations of the samples were $x = 0.19, 0.41,$ and 0.60. We will neglect this and compare to the nominal values of 0.25, 0.5, and 0.7.